Erschienen in: 2012 38th IEEE Photovoltaic Specialists Conference. - IEEE, 2012. - S. 001584-001589
https://dx.doi.org/10.1109/PVSC.2012.6317897

Effects of Process Conditions for the n^+-Emitter Formation in Crystalline Silicon

A. Dastgheib-Shirazi[1], M. Steyer[1] G. Micard[1], H. Wagner[2], P. Altermatt[2], and G. Hahn[1]

[1]Department of Physics, University of Konstanz, 78457 Konstanz
[2]Dep. Solar Energy, Inst. Solid-State Physics, Leibniz University of Hannover, 30167 Hannover, Germany

***Abstract* — Nowadays new solar cell concepts are continually attracting the attention of the PV industry. Thereby emitter structures and the application of high performance emitters like the homogeneous and etched-back emitter on crystalline p- and n-type silicon solar cells continue to be very popular [1]-[4]. In this work we study the influence of process parameters on the phosphosilicate glass layer characteristics during the predeposition of a $POCl_3$ diffusion process. The quantitative analysis of the highly doped layer gives a deeper understanding of the phosphorus diffusion process for industrial emitter structures.**

Index Terms —Emitter, $POCl_3$-Diffusion, PSG, Simulation

I. Introduction

In general practice, n^+-emitters are usually produced using a high temperature diffusion process, whereby it is popular for this purpose to use a $POCl_3$ diffusion process. Hereby the concentration profile of P in Si can be fairly precisely adjusted by manipulating the large number of process parameters. This work is focused on the first phase of the diffusion process, in which a highly doped phosphosilicate glass (PSG) layer grows and serves as a source for subsequent P diffusion in Si. Quantitative measurements of this highly doped layer make it possible to quantify growth characteristics and layer composition as a function of process parameters. The thereby acquired information helps to expand the existing mathematical models for the simulation of P diffusion in Si [5]-[9].

A. Emitter Formation

For most solar cell concepts the emitter area consists of a relatively thin highly doped layer on the front side of the solar cell. In general, we differentiate fundamentally between a homogeneous and a heterogeneous emitter. With homogeneous emitters the highly doped layer is embedded in the same material as the base. The heterogeneous emitter concept consists, to the contrary, of two different materials for emitter and base [10]. Before turning to the fabrication of emitters by means of diffusion, let us consider four alternatives.

Ion implantation of P into Si offers a possibility to create a highly doped region [11]. After the implantation step the samples are annealed at high temperatures in order to heal defects in the crystal lattice. The advantages of this method are the precise adjustment of the concentration profile and the absence of the PSG layer. On the other hand, the absence of the PSG layer may reduce the external gettering effect.

The second alternative to the diffusion process is the emitter formation by epitaxial growth using CVD (chemical vapour deposition) at temperature ranges >1000°C [12]. The highly doped layer thereby grows with a very high growth rate (30 times faster than the $POCl_3$ diffusion process). Thereby epitaxially grown emitters reach surface P concentrations of about $1\text{-}2\cdot10^{19}$ cm^{-3}. These low P concentrations significantly reduce the emitter recombination rate. However, these emitters can not yet be contacted to industrial standards by means of screen printing procedures.

A further alternative to emitter fabrication is the heterojunction structure. The principle is thereby based on the combination of a crystalline silicon layer with a doped amorphous Si layer with opposed doping. Through the employment of a further intrinsic amorphous Si layer an excellent passivation quality can be achieved with V_{oc} values above 700 mV [13]. The advantages of the low process temperature and the high passivation quality are, however, offset by the complex wet chemical processing of the wafers and the more difficult contact formation in the low temperature range (<300°C).

An entirely different way to fabricate a pn-junction is the formation of an inversion layer between a metal and an insulator. The thin inversion layer that arises thereby has a high number of fixed positive charges, whereby there is a significant increase in the electron density on the interface between the insulator and the silicon. This is consistent with the fact that the electrons on the silicon surface become majority charge carriers, as is also the case with an n-type emitter. The inversion layer has the advantage over the diffusion process that through the low process temperatures it displays very low saturation current densities. However, as well here the contact formation is also more difficult. Similar to the case with the ion implanted emitter, due to the low process temperatures and the absence of a PSG layer there are no gettering effects.

In this work we concentrate on a high temperature diffusion process, as represented by the $POCl_3$ diffusion. The $POCl_3$ emitter diffusion process carried out in a quartz tube offers a much larger range of process parameters for a precise adjustment of the process parameters during P diffusion in Si than e.g. an inline diffusion process.

This diffusion process is generally divided into two phases. In the first phase, which is called predeposition, a highly doped PSG is formed on and in the Si substrate. During the diffusion process this layer serves as a source of dopant for P diffusion, and depending on the diffusion parameters it can be regarded as either a finite or an infinite source. This distinction depends strongly on the choice of process parameters during the diffusion process.

The main process parameters that can be adjusted during predeposition are duration, temperature, $POCl_3$-N_2 flow and O_2 flow. After predeposition follows the drive-in step, during which no $POCl_3$-N_2 flow takes place. In this phase the P already diffused into the Si is driven further in. Next comes the cool-down process, which has great relevance for gettering effects [14]. In this study we will, however, mainly concentrate on predeposition, whereby the analysis of the PSG layer is the central focus.

This allows for a better understanding of the mechanisms of P diffusion in crystalline silicon. Such quantitative analyses of the PSG layer also simultaneously expand the boundary conditions for the simulation of P diffusion in Si using TCAD [7].

Another focal point of this work is the analysis of the influence of the process gasses during P diffusion on the concentration of the active and inactive P in the Si and thereby on the electrical performance of those emitter structures. The main process gasses $POCl_3$-N_2 and O_2 have a decisive influence on the emitter profile, especially on the surface concentration and on the characteristic plateau. We will deal in this work with the dependency of the electrical characteristics of the emitter on the process gasses during P diffusion. Later, the connection between P concentration and contactability of screen printed solar cells will be dealt with.

II. PSG Formation

The goal of this study is to make a comparison between a measured and a simulated P concentration profile. From this it becomes clear that a quantitative PSG analysis (in particular the determination of the layer thickness and the trend of P concentration in the PSG) enables us to set more realistic boundary conditions for the simulation of P diffusion in Si.

In the experiments presented in this work, a commercial open tube $POCl_3$ diffusion furnace from Centrotherm is used. The selection of the samples and the process parameters are explained in detail in the discussions of the particular experiments. In the following diagram the $POCl_3$ diffusion process is schematically represented.

In the experiments presented in this work, a commercial open tube $POCl_3$ diffusion furnace from Centrotherm is used. The selection of the samples and the process parameters are explained in detail in the discussions of the particular experiments. In the following diagram the $POCl_3$ diffusion process is schematically represented.

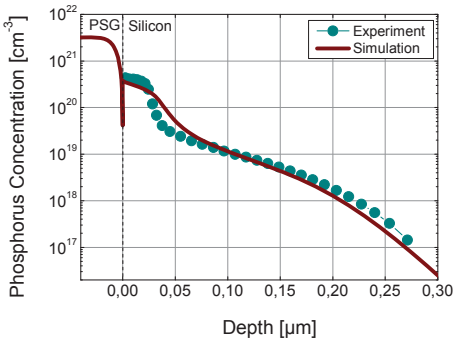

Fig. 1 Comparison between measured ECV profile of a diffused emitter and P concentration profile calculated by process simulation [7].

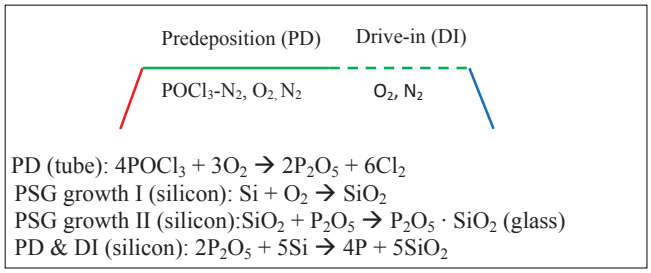

Fig. 2. Overview of the $POCl_3$ diffusion process.

In the first part of this work methods for quantitative analysis of the PSG layer are presented. The emphasis will hereby be on the growth behavior of the PSG layer. Thereby not only layer thickness, but also layer composition is of great importance. In order to specifically capture the PSG growth behavior, we consider in the following experiments only the predeposition. To determine the exact PSG layer thickness, mirror polished samples were measured using atomic force microscopy (AFM) and spectroscopic ellipsometry measurements. The following diagram shows the measured PSG layer thickness in dependence on the $POCl_3$-N_2/O_2 ratio during predeposition. The material for the experiment consisted of <100> oriented, 2 Ωcm, p-type FZ Si wafers with a thickness of 220 µm. After cleaning, the wafers were diffused at 840°C for 40 min.

The increase in PSG layer thickness in Fig. 3 shows almost a saturation with an increased $POCl_3$-N_2/O_2 flow ratio.

The following experiment is again devoted to the predeposition phase. The question arises of the extent to which the oxygen flow influences the PSG layer thickness and the P concentration profile in Si. The material for this experiment consisted of <100> oriented, 2 Ωcm, p-type FZ Si wafers. After cleaning, these wafers were diffused with the same process temperature of 840°C, a predeposition duration of 40 min and a constant $POCl_3$-N_2 flow, but with variations in the O_2 flow.

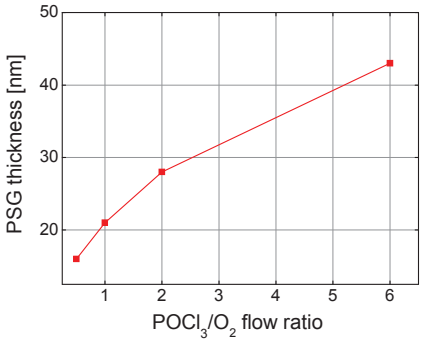

Fig. 3. Measurements of the PSG thickness using AFM.

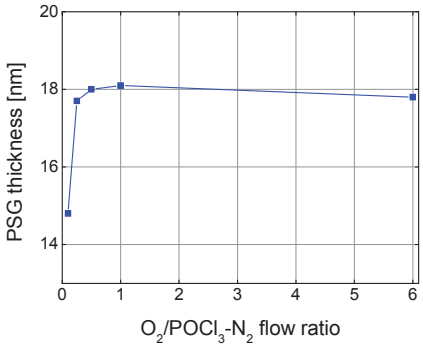

Fig. 4. PSG thickness as a function of O_2 flow during predeposition.

The increase in the O_2 flow for $O_2/POCl_3$-N_2 ratios above 0.25in Fig. 4 during predeposition, in this experiment, already starting at an $O_2/POCl_3$-N_2 ratio of 0.25 has no further influence on the PSG layer thickness as shown in Fig. 4. This confirms that already small amounts of oxygen in comparison to standard process conditions in the diffusion furnace are sufficient for the creation of the PSG. However, here we can still not yet reach any conclusions about the ratio between $P_2O_5 \cdot SiO_2$ and SiO_2 in the PSG, since with the analytical methods for determining the layer thicknesses the borders of the two components in the PSG are still not clearly distinguishable.

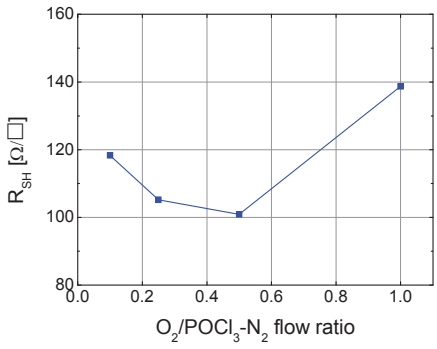

Fig. 5. R_{sheet} in dependence on the O_2 flow during predeposition.

In Fig. 5 we see the trend of the sheet resistance R_{sheet} in dependence on the O_2 flow during predeposition. From this we can infer that with increasing O_2 flow R_{sheet} decreases. However, R_{sheet} rises again if the $O_2/POCl_3$-N_2 flow ratio reaches values above 0.5. In order to examine this more closely, in the following we examine the trend of the electrically active P.

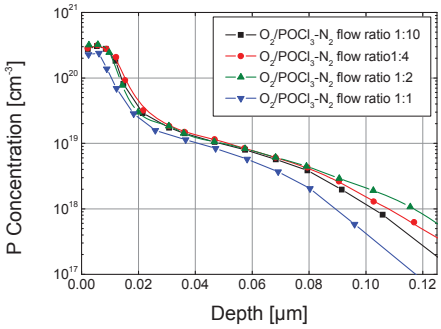

Fig. 6. ECV measurements of the n-type emitter after predeposition with variations of the O_2 flow.

Fig. 6 shows the influence of the increase in O_2 flow during predeposition as a function of the electrically active P concentration in Si measured by electrochemical capacitance voltage (ECV). The increased O_2 concentration during predeposition causes a slight reduction in the electrically active P concentration close to the surface. If we regard the plateau depth of the emitter up to $1 \cdot 10^{20}$ cm^3, the increase in the O_2 flow causes a significant reduction of the plateau depth. Also in the tail region, which reflects the initial state of the predeposition phase, there is a correlation between the concentration profile and the O_2 content. We can assume that the initial oxidation increases the diffusivity of P in Si. This effect is especially apparent in the tail region of the emitter profile [15].

If the O_2 flow exceeds that of the $POCl_3$-N_2 flow, then we can assume that the initial SiO_2 layer thickness grows at a higher rate and thereby acts during diffusion as a diffusion barrier. This would explain why the sheet resistance in Fig. 5 begins to rise again with an $O_2/POCl_3$-N_2 flow ratio approaching unity.

III. Total Phosphorus Amount (Q) in PSG

With PSG analysis an interesting question is the total amount of P is in this layer. In addition, it is very important for the diffusion process to know whether the PSG is depleted during the diffusion process. The P dose can be directly determined using inductively coupled plasma optical emission spectrometry (ICP-OES) measurements, whereby the PSG is dissolved in HF and quantitatively analyzed.

To answer the question whether the PSG is depleted after a long annealing step at a temperature of 940°C for 6 h in N_2

atmosphere, the total amount of P in the PSG layer was measured using ICP-OES.

The samples in this experiment were first diffused at a temperature of 840°C and a predeposition duration of 40 min. As can be seen from Fig. 7, the total P dose (Q) in the PSG layer increases with increasing $POCl_3$-N_2 flow. However, we must remember that the increase in the $POCl_3$-N_2 flow causes an increase in layer thickness.

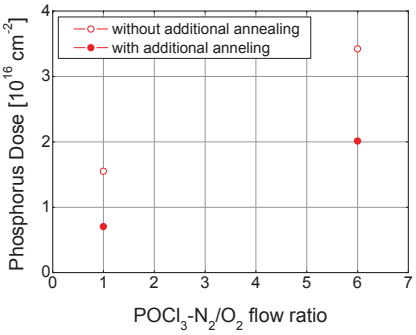

Fig. 7. ICP-OES measurements of the total P dose Q of PSG layers depending on the $POCl_3$-N_2 flow during predeposition. Closed circles represent samples annealed after predeposition in N_2 atmosphere at a temperature of 940°C for 6 h.

Taking into account the already measured PSG layer thickness for this $POCl_3$ flow variation, we obtain a range for the maximum P concentration in the PSG of between $7.40 \cdot 10^{21}$ and $7.95 \cdot 10^{21}$ cm^{-3}. A further interesting conclusion from Fig. 7 is that after annealing the samples at 940°C for 6 h the total dose of P in the PSG is reduced but far from depleted.

IV. Reduction of Phosphorus Precipitates

The ECV profile shows the electrically active P, from which the emitter sheet resistance results. If we compare several emitters diffused under differing process conditions with the same sheet resistance R_{sheet}, the difference in the emitter saturation current density j_{0E} of these emitters cannot be attributed primarily to the active surface concentration and thereby to Auger recombination. As is already known, highly doped industrial emitters show P concentrations on the emitter surface above the solubility limit and in the surface-near emitter volume. Precisely these precipitates play a decisive role in the reduction of minority charge carrier lifetime in the emitter bulk. It can definitely be assumed that a reduction in the density of these precipitates leads to a reduction of the emitter saturation current density. A direct comparison of the profiles of the electrically active P with the overall concentration of P seems to resolve this discrepancy.

For this experiment we employed chemically etched <100> oriented, p-type FZ wafers with a nominal resistivity of 2 (for ECV) and 200 Ωcm (for j_{0E}) and a thickness of 220 µm.

After cleaning, the samples were diffused under different process gas conditions, whereby the $POCl_3$-N_2 gas flow was varied, while the O_2 flow was kept constant. Thereby it was made sure that each sample displayed the same sheet resistance of 48 Ω/sq. This was ensured through a moderate temperature adjustment.

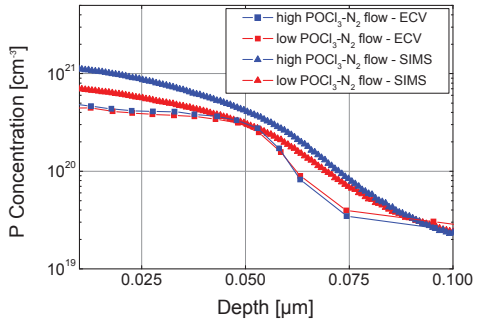

Fig. 8. SIMS and ECV profiles of two emitters diffused under high and low $POCl_3$-N_2 flows during predeposition.

After the diffusion process and the PSG etching, the samples with a nominal resistivity of 200 Ωcm were coated on both sides with plasma enhanced chemical vapor deposited SiN_x fired in a belt furnace, and the emitter saturation current density j_{0E} was measured using quasi steady state photoconductance in high injection conditions. In this case the measured j_{0E} difference of the two emitters in Fig. 8 is about 90 fA/cm². In order to find the reason for this difference we compare the concentration profiles of the electrically active with the overall P. In a comparison of the active P of the emitters with the low and high $POCl_3$-N_2 flow it becomes clear that the $POCl_3$-N_2 variation has no significant influence on the ECV profile. In contrast, the comparison of the secondary ion mass spectroscopy (SIMS) profiles in Fig. 8 shows an increase in the chemical concentration with increased $POCl_3$-N_2 flow. Here the influence of the $POCl_3$-N_2 variation on the reduction of j_{0E} is less attributable to differences in the electrically active P. Rather, through the reduction of the $POCl_3$-N_2 flow the density of P precipitates is reduced. This causes a reduction of the Shockley-Read-Hall recombination in the emitter bulk, which increases the effective minority lifetime in the emitter bulk near the surface. The reduction of the $POCl_3$-N_2 flow leads, as can be seen in Fig. 9, to a reduction of the chemical surface concentration of P in the surface-near emitter bulk. The threshold where the concentration of the inactive P equals the concentration of the active P was in this experiment reached at a $POCl_3$-N_2/O_2 ratio of 1.

This reduction of the electrically inactive P also plays an important role in the contact formation of such emitters by means of the screen printing technique. Solar cell results show that the contact resistance of screen printed solar cells with a homogeneous emitter increases significantly exactly where the

difference in concentration between the inactive and the active P is eliminated (see Fig. 9). This also means, however, that through the adaptation of the $POCl_3$-N_2 flow during predeposition up to that range, with constant low contact resistance the saturation current density j_{0E} of the emitter can be reduced. This experiment can be summarized as follows: The reduction of the $POCl_3$-N_2 flow with simultaneous temperature adaptation has the effect that the electrical performance of a homogeneous emitter can be significantly improved, although all the emitters studied here display the same R_{sheet} of 48 Ω/sq.

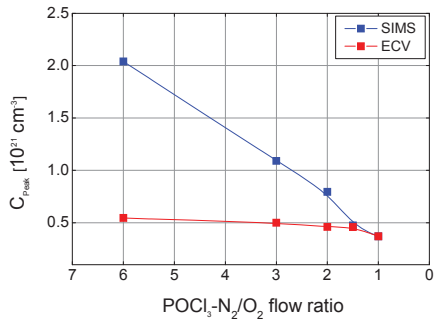

Fig. 9. Comparison of the maximal surface concentration of P determined from SIMS and ECV measurements. The samples were diffused under several $POCl_3$-N_2 gas flow conditions. The predeposition temperature was adjusted to achieve the same sheet resistance of 48 Ω/sq on all samples.

In the next experiment we consider the above described $POCl_3$-N_2 flow variation at the constant predeposition temperature of 840°C. Here we wanted to determine the extent to which the ratio of $POCl_3$-N_2/O_2 has effects during predeposition on the j_{0E} and implied V_{oc} values of the emitter. In Fig. 10 we see the trend of the j_{0E} and additionally implied V_{oc} values in dependence on the gas flow. As in the last experiment, the reduction of the $POCl_3$-N_2 flow leads to a sharp reduction of j_{0E} and a significant gain in the implied V_{oc} values. In order to explain the improvement of the electrical performance of the emitters, first of all we consider the concentration of the electrically active P. Here it becomes clear, first, that the reduction of the $POCl_3$-N_2 flow has hardly any influence on the maximum surface concentration. However, we see in the same Fig. 11 that with a falling $POCl_3$-N_2 flow the plateau depth (up to $1 \cdot 10^{20}$ cm^{-3}) of the emitter becomes thinner. In contrast to the last experiment, here the process temperature was kept constant at 840°C, so that the gas flow variation had a direct significant influence on the plateau depth and thereby on R_{sheet}.

The measured surface concentration of the active P is almost independent from the $POCl_3$ flow. Only a ratio of 1:1 between $POCl_3$-N_2 and O_2-flow appears to significantly reduce not only the plateau depth, but also the surface concentration. This can be related to the fact that during the first phase of predeposition the SiO_2 layer of the PSG develops more strongly and works as a weak diffusion barrier. The profiles of the chemical P concentration in Fig. 12 show in addition to the reduction of the plateau depth with falling $POCl_3$-N_2 flow as well a significant reduction of the surface concentration, in contrast to the ECV profiles in Fig. 11. The comparison of the two diagrams makes clear that with falling $POCl_3$-N_2 flow during predeposition the surface concentration of the active P approaches that of the overall P concentration.

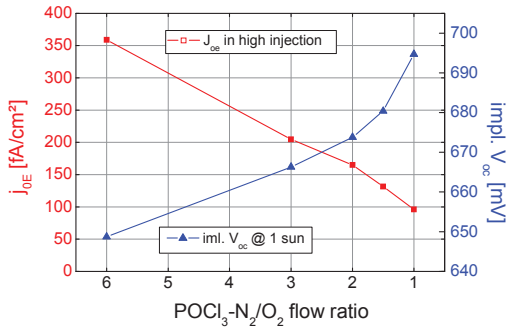

Fig. 10. j_{0E} and impl. V_{oc} measurements of symmetrical samples in dependence on the $POCl_3$-N_2/O_2 flow ratio during predeposition at a temperature of 840°C.

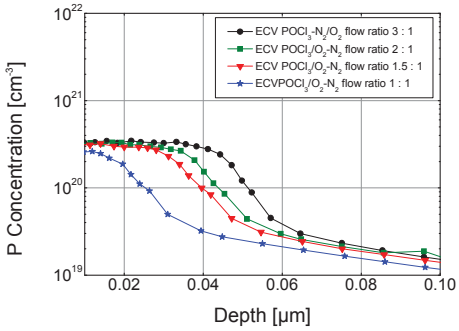

Fig. 11. ECV profiles of the active P concentration as a function of the $POCl_3$-N_2 /O_2 flow.

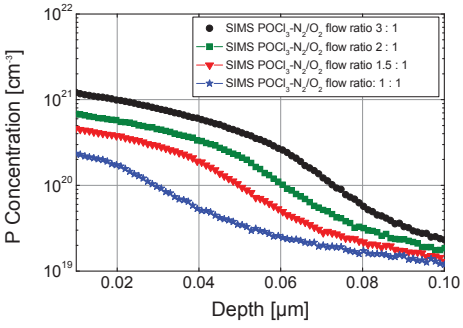

Fig. 12. SIMS profiles of the chemical P concentration in dependence of the $POCl_3$-N_2 flow during predeposition.

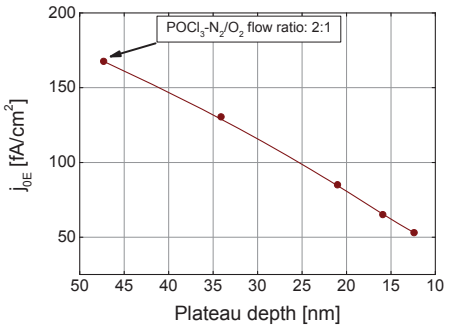

Fig. 13. j_{0E} measurements on etched back emitters in dependence on the plateau depth (up to $1 \cdot 10^{20}$ cm^{-3}).

Fig. 13 shows j_{0E} values for several etched-back emitters. This demonstrates that a further reduction of j_{0E} down to 50 fA/cm² can be reached using controlled wet chemical emitter etching [1].

We can conclude from the two previous experiments that the reduction of the $POCl_3$-N_2 flow during the predeposition phase improves the electrical performance of the emitters, above all due to the reduced Shockley-Read-Hall recombination in the surface-near emitter bulk. With a solar cell process, such an adaptation of the gas flow would drastically increase the trend of the internal quantum efficiency in the short wavelength area. This would lead to a gain in V_{oc} and j_{sc}, providing sufficient contacting of the solar cell is assured with the screen printing procedure.

A further important point is that an emitter with reduced P precipitation also allows improved emitter passivation by extended dielectric passivation layers [2].

The combination of an n-type emitter on p-type silicon [1, 4], as well as the combination of an n-type FSF on an n-type substrate [4] which features reduced P precipitates with the selective emitter etched-back concept makes possible further increases in efficiency on large area screen printed solar cells.

V. Conclusion And Outlook

This work was focused on the first stage of the $POCl_3$ diffusion process. In the first experiments we have shown quantitative analyses with regard to the PSG thickness and the total amount of P in the PSG. Furthermore, this work dealt with the influence of the $POCl_3$-N_2 flow during predeposition. The correlation between the $POCl_3$-N_2 flow and enhanced clustering effects has also been studied. In the next step we will study the influence of process parameters during the predeposition and the drive-in phase on the properties of the PSG layer and its composition. The results will be transferred as boundary conditions to numerical simulation of P diffusion in Si including the PSG as the dopant source.

Acknowledgement

The basic project for parts of this report was financially supported by our industry partners centrotherm photovoltaics AG and SolarWorld Innovations. We also would like to thank R. Chen and S. Dunham for the scientific cooperation. The financial support from the BMU project FKZ 0325079 is gratefully acknowledged in particular for the characterization equipment.

References

[1] A. Dastgheib-Shirazi et al., "Selective emitter for industrial solar cell production: a wet chemical approach using a single side diffusion process," in *23rd EU PVSEC,* 2008, p. 1197.

[2] A. Dastgheib-Shirazi et al., "Investigations of high refractive silicon nitride layers for etched back emitters: enhanced surface passivation for selective emitter concept (SECT)," in *24th EU PVSEC,* 2009, p. 1600.

[3] G. Hahn, "Status of selective emitter technology," in *25th EU PVSEC,* 2010, p. 1091.

[4] F. Book et al., "Analysis of processing steps for industrial large area n-type solar cells with screen printed aluminum-alloyed rear emitter and selective FSF," in *26th EU PVSEC,* 2011, p. 1160.

[5] R. Chen, "Understanding coupled oxide growth and phosphorus diffusion in $POCl_3$ deposition for control of phosphorus emitter diffusion," this conference

[6] S.T. Dunham, "A quantitative model for the coupled diffusion of phosphorus and point defects in silicon," *J. Electrochem. Soc.* vol. 139, pp. 2628-2635, 1992.

[7] H. Wagner et al., "Improving the predictive power of modeling the emitter diffusion by fully including the phosphosilicate glass (PSG) layer," in *37th IEEE PVSC,* 2011, p. 2957.

[8] H. Wagner, "Analyzing emitter dopant inhomogeneities at textured Si surfaces by using 3D process and device simulations in combination with SEM imaging," this conference

[9] G. Micard et al., "Diffusivity analysis of $POCl_3$ emitter SIMS profiles for semi empirical parameterization in Sentaurus process," in *26th EU PVSEC,* 2011, p. 1446.

[10] E. Maruyama et al., "Sanyo's challenges to the development of high-efficiency HIT solar cells and the expansion of HIT business," in *WCPEC-4,* 2006, p. 1455.

[11] J. W. Mayer et al., Ion implantation in semiconductors: silicon and germanium, Academic Press, Inc., 1970.

[12] E. Schmich, High-Temperature CVD processes for crystalline silicon thin-film and wafer solar cells, PhD thesis, University of Konstanz, 2008.

[13] A. Aberle, "Progress in low-temperature surface passivation of silicon solar cells using remote-plasma silicon nitride," *Progr. Photovolt.: Res. Appl.*, vol. 5, pp. 29–50, 1997.

[14] J. Schön et al., "Understanding the distribution of iron in multicrystalline silicon after emitter formation: theoretical model and experiments," *J. Appl. Phys.*, vol. 109, pp. 063717, 2011.

[15] G. Masetti et al., "On phosphorus diffusion in silicon under oxidizing atmospheres," *Solid-State Electronics*, vol. 16, pp. 1419-1421, 1973.